ISSN 0023-1584, Kinetics and Catalysis, 2008, Vol. 49, No. 4, pp. 506–514. © MAIK "Nauka/Interperiodica" (Russia), 2008.
Original Russian Text © G.A. Kovalenko, T.V. Chuenko, N.A. Rudina, L.V. Perminova, 2008, published in Kinetika i Kataliz, 2008, Vol. 49, No. 4, pp. 529–538.

Preparation and Characterization of Supports with a Synthesized Layer of Catalytic Filamentous Carbon: III. Synthesis of Carbon Nanofibers on Nickel Supported onto Aluminum Oxide

G. A. Kovalenko, T. V. Chuenko, N. A. Rudina, and L. V. Perminova

Boreskov Institute of Catalysis, Siberian Branch, Russian Academy of Sciences, Novosibirsk, 630090 Russia
e-mail: galina@catalysis.ru

Received June 20, 2007

Abstract—The synthesis of catalytic filamentous carbon (CFC) on catalysts prepared by supporting Ni^{2+} compounds onto the surface of various alumina modifications (macroporous α-Al_2O_3 and mesoporous θ-Al_2O_3 and δ-Al_2O_3) using two procedures (impregnation and homogeneous precipitation) was studied. The texture characteristics (specific surface area and pore structure) of the parent supports and adsorbents with a CFC layer were compared. The effect of the supporting procedure on the surface morphology of Ni/Al_2O_3 catalysts and the synthesized CFC layer was studied by scanning electron microscopy. It was found that the carbon yield on a macroporous catalyst prepared by homogeneous precipitation was higher than that on a catalyst prepared by impregnation by a factor of ~2. The CFC layer exhibited a mesoporous structure because of a chaotic interlacing of carbon nanofibers, and the synthesis of CFC on macroporous supports resulted in the formation of a bidisperse pore structure of the adsorbent. Active and stable heterogeneous biocatalysts were prepared by the adsorptive immobilization of enzymatically active substances (glucoamylase and nongrowing baker's yeast cells) on CFC.

DOI: 10.1134/S0023158408040083

INTRODUCTION

Nanoporous carbon–mineral composite materials have attracted increasing attention as selective adsorbents and catalysts or specific catalyst supports, as well as engineering materials for special operating conditions (fuel cells), in the past few decades.

It is well known that iron subgroup metals (cobalt and nickel) and copper are the most active catalysts for the synthesis of carbon nanofibers by a carbide mechanism [1–3]. It was found that the structure of carbon filaments (the mutual arrangement of the graphene planes with respect to the fiber axis) and the morphology of a synthesized catalytic filamentous carbon (CFC) layer depend on the nature of the supported metal catalyst, the metal particle size [2, 4], and the conditions of the carbon layer synthesis (the nature of the starting hydrocarbon raw material, the composition of the hydrocarbon-containing gas mixture, and the temperature of pyrolysis) [1, 5, 6].

Nickel-containing catalysts for the production of a carbon adsorbent as rounded granules with a specific surface area of ≥200 m^2/g (bulk CFC) formed by a chaotic interlacing and significant compacting of carbon nanofibers are prepared by either the coprecipitation of nickel and aluminum hydroxides [5, 7, 8] or the mechanochemical activation of corresponding powdered metal oxides and hydroxides [1].

Recently, attention has been focused on the synthesis of a thin CFC layer (1–5 μm) on the surfaces of inorganic supports with the retention of their intricate geometric shapes and mechanical strengths; this considerably extends the range of materials for various practical applications. For example, de Lathouder et al. [9, 10] described ceramic honeycomb monoliths with a synthesized CFC layer, which were proposed as new macrostructured reactor–adsorbent materials for immobilized enzymes (lactase and lipase). Vieira et al. [6] prepared a new composite material—CFC on graphite; plates and rings of various sizes were made of this material for the use in catalytic reactors. Both impregnation [6] and homogeneous precipitation in the presence of urea [9, 10] are used for supporting Ni compounds onto support surfaces.

The aim of this work was to perform a comparative study of the effect of methods used for supporting Ni^{2+} compounds onto the surfaces of various Al_2O_3 modifications (α-, θ-, and δ-Al_2O_3) upon the following texture and physicochemical characteristics of the resulting adsorbents with a CFC layer: the specific surface area (S_{sp}), the pore structure, and the carbon yield ((g carbon)/(g nickel)). The goal was also to study the morphology of CFC layers synthesized on the surfaces of Ni catalysts prepared by impregnation and homogeneous precipitation using scanning electron microscopy and to examine the adsorptive immobilization of the enzyme glucoamylase and nongrowing baker's

yeast cells for the preparation of heterogeneous biocatalysts for the hydrolysis of dextrin and the inversion of sucrose.

EXPERIMENTAL

The following alumina modifications were used as parent supports for the supporting of Ni^{2+} compounds and the synthesis of CFC: δ-Al_2O_3 (S_{sp} = 82 m^2/g) as rods 5–7 mm in length and 2 mm in diameter; θ-Al_2O_3 (S_{sp} = 55 m^2/g) as rings 2–5 mm in height and 4–5 and 1.5–2 mm in inner and outer diameters, respectively; and α-Al_2O_3 (S_{sp} = 0.5 m^2/g) as rings 5–6 mm in height and 7 and 2 mm in inner and outer diameters, respectively. A corundum honeycomb monolith (S_{sp} = 5.5 m^2/g) as cylinders ~2 cm in length and ~0.9 cm in outer diameter with channels of ~0.9 × 0.9 mm square section (number of channels, 37), which was prepared by extrusion molding and calcined at 1100°C, was also used.

Nickel compounds were supported onto the surfaces of parent supports by (1) impregnation from a solution of nickel nitrate (0.01 mol/l) and (2) homogeneous precipitation from a solution containing nickel nitrate (0.01 mol/l) and urea (0.1 mol/l). The parent supports (1 part by weight) were placed in the prepared solutions (~5 parts by volume), heated in a water bath to 85 ± 1°C, and kept for 3 h at the specified temperature. The resulting Ni/Al_2O_3 catalysts were washed with distilled water and dried under an IR lamp for 4–6 h. The dried catalysts were cooled and kept in a desiccator with KSK silica gel. The concentration of nickel (wt %) was determined by atomic absorption spectrometry on an ASSIN instrument with a flame-ionization detector.

The synthesis of CFC was performed by the pyrolysis of a hydrogen–propane–butane gas mixture at 500°C. The fixed catalyst bed was formed using a stainless steel gauze cylindrical insert, which was placed in a horizontally arranged quartz tube reactor 200 mm in length and 30 mm in diameter. The temperature of the furnace with the reactor was maintained using a PROTERM-100 microprocessor regulator. In the reactor, Ni/Al_2O_3 (10–20 g) was additionally dried in a flow of nitrogen (12 l/h) at 85°C for 30 min; then, the flow of nitrogen was replaced by a flow of a gas mixture containing hydrogen (3 l/h) and propane–butane (24 l/h). The reactor temperature was increased to 500°C at a rate of 10 K/min, and the pyrolysis of hydrocarbons was performed for 1 h.

The amount of carbon (wt %) synthesized on Ni/Al_2O_3 was determined gravimetrically from either (i) an increase in the weight in the course of pyrolysis or (ii) a decrease in the weight upon annealing at 800°C for 3 h. In calculation procedure (i), the starting point was the weight of Ni/Al_2O_3 dried under an IR lamp for 4–6 h. In calculation procedure (ii), the starting point was the weight of the CFC/Ni/Al_2O_3 adsorbent removed from the reactor and cooled in a desiccator. It was found that, for calcined macroporous supports (corundum and ceramic honeycomb monoliths), the amounts of synthesized carbon measured from an increase (pyrolysis) or decrease (annealing) in the weight were consistent within the limits of experimental error (1–2%). In the calculations of carbon contents, the hygroscopicity of supports, which was evaluated upon drying at 200°C for 4 h to constant weight, was taken into consideration. It was found that macroporous supports based on α-Al_2O_3 were nonhygroscopic, whereas the hygroscopicity of mesoporous θ-Al_2O_3 and δ-Al_2O_3 was, on average, 2.2%.

The productivity of the synthesis of CFC was characterized by the carbon yield (Y), which is equal to the weight (g) of synthesized carbon per gram of supported nickel.

The specific surface areas (S_{sp}) of supports were measured using the thermal desorption of argon on a SORBI-M instrument (ZAO Meta, Russia). The pore-size (d_{pore}) distribution was determined by mercury porosimetry on an AUTO-PORE 9200 Instrument (Micromeritics, United States).

The electron-microscopic studies of the surfaces of Ni catalysts and the morphology of a synthesized carbon layer were performed with the use of JSM 6460 LV (JEOL, Japan) and LEO 1430 (LEO, Germany) scanning electron microscopes. Marks in micrographs indicate distances in μm.

The resulting adsorbents with a CFC layer were used for the immobilization of the enzyme glucoamylase, which exhibits catalytic activity in the hydrolysis of dextrin, as well as for the immobilization of nongrowing baker's yeast cells with invertase activity. Conditions for the determination of glucoamylase and invertase activity, as well as conditions for the adsorptive immobilization of the enzyme and microorganisms, were described elsewhere [11, 12]. The enzymatic activity was expressed in terms of μmol of glucose formed at 50°C in 1 min per 1 mg of protein or 1 mg of dry cells for the enzyme in solution or microorganisms in suspension, respectively. The activity of a heterogeneous biocatalyst was expressed in μmol/min per gram of biocatalyst. The experimental error was no higher than 15%.

The stability of the resulting heterogeneous biocatalysts was determined by keeping them in a buffer solution (a 0.05 M acetate buffer, pH 4.6) at 18–20°C and measuring the residual activity at regular intervals. For long-term storage (more than two months), 0.02% sodium azide was added to the buffer solution.

RESULTS AND DISCUSSION

δ-Alumina and θ-Alumina (Rods and Rings)

The concentrations of nickel supported by procedures 1 and 2 on the surface of mesoporous Al_2O_3 were equal: 0.16 ± 0.02 wt %. The main differences were found using electron microscopy. After impregnation,

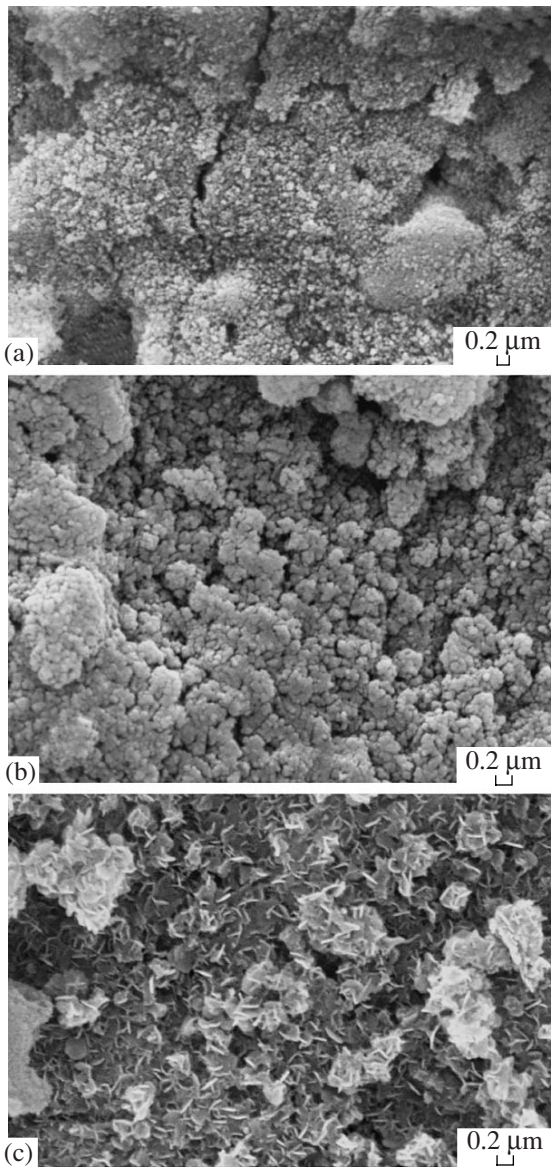

Fig. 1. Electron-microscopic images of the surface of mesoporous δ-Al_2O_3 (rods): (a) the parent support, (b) the support with 0.16% Ni supported by impregnation, and (c) the support with 0.15% Ni supported by homogeneous precipitation.

the surface of the parent Al_2O_3 (Fig. 1a) was smoothed with the retention of the initial relief and no coarse particles of nickel compounds were detected (Fig. 1b). Upon homogeneous precipitation, relatively coarse flaky particles of nickel hydroxide were detected (Fig. 1c). In both cases, the S_{sp} of supports containing Ni^{2+} compounds increased by 10–20%.

In a visual examination of mesoporous alumina granules with synthesized CFC and their cleavages, we found that, when the Ni/Al_2O_3 catalyst was prepared by impregnation, carbon deposits were uniformly distributed across the entire granule and the entire rods of δ-Al_2O_3 were intensely black. In the preparation of the Ni/Al_2O_3 catalyst by homogeneous precipitation, the synthesis of CFC occurred nonuniformly across a granule: the formation of an intensely black external crust region 0.2–0.3 mm in depth (~10% of the rod diameter) on δ-Al_2O_3 rods was observed, whereas the internal region of the granule was light gray. Evidently, these differences were due to the particle sizes of supported nickel compounds (Fig. 1). It is likely that larger nickel hydroxide particles, which were formed in a solution of nickel nitrate in the presence of urea, did not penetrate into the inner space of granules of mesoporous δ-Al_2O_3 because of diffusion hindrances; they were mainly deposited onto the external surface. In the synthesis of the CFC layer, the S_{sp} of parent mesoporous supports increased by ~20–30% and the carbon yield was no higher than 10 g/g (Table 1).

Note that mesoporous δ-Al_2O_3 and θ-Al_2O_3 (with no supported Ni) exhibited an insignificant catalytic activity in the pyrolysis of a H_2–propane–butane mixture. The pyrolytic carbon contents of the supports were 0.9 and 0.8%, respectively. As noted above, it is likely that this resulted in the appearance of a light gray color in the inner region of the granules.

An electron-microscopic examination did not exhibit differences between the surfaces of the parent Al_2O_3 (Fig. 2a) and carbonized Ni/Al_2O_3 prepared by impregnation (Fig. 2c). As mentioned above, nickel compounds supported by impregnation did not form coarse particles on the surface of alumina (Fig. 1b) and the carbon layer synthesized on this catalyst resembled the morphology of the parent support (Fig. 2c). A comparison between electron micrographs in Figs. 2b and 2d indicates that the surface of the carbonized parent θ-Al_2O_3 support (without Ni) was smoother than the surface of the CFC-containing Ni/Al_2O_3 prepared by homogeneous precipitation. However, carbon deposits did not exhibit a pronounced nanofiber structure (Fig. 2d).

Thus, a comparison between the two procedures for supporting nickel onto the surface of mesoporous alumina demonstrated that the main difference was in the character of synthesized carbon distribution across the support granule. Homogeneous precipitation was characterized by a nonuniform carbon layer because carbon was synthesized in a region adjacent to the surface of a granule because of the formation of coarser Ni particles and the resulting adsorbents exhibited a crust structure.

α-Alumina (Rings and Honeycomb Monoliths)

A comparison between the two procedures for supporting Ni^{2+} compounds onto the surface of macroporous Al_2O_3 modifications demonstrated that the nickel content upon homogeneous precipitation was greater than that upon impregnation by a factor of ~2 (Table 1). Using scanning electron microscopy, we detected relatively coarse particles of nickel compounds on the parent support surfaces (Figs. 3a, 3c).

Table 1. Physicochemical properties of carbon-containing adsorbents depending on the procedure used for supporting nickel compounds onto aluminum oxides

Parameter	α-Al_2O_3 rings (S_{sp} = 0.5 m^2/g)		α-Al_2O_3 honeycomb monolith (S_{sp} = 5.5 m^2/g)		θ-Al_2O_3 rings (S_{sp} = 55 m^2/g)		δ-Al_2O_3 rods (S_{sp} = 82 m^2/g)	
	impregnation	homogeneous precipitation	impregnation	homogeneous precipitation	impregnation	homogeneous precipitation	impregnation	homogeneous precipitation
Ni, wt %	0.06	0.11	0.17	0.27	0.15	0.18	0.19	0.16
C, wt %	3.0	8.4	2.9	8.1	1.2	1.1	0.9	1.4
Carbon yield, C/Ni, g/g	49.2	76.2	17.1	30.0	8.1	6.3	4.3	8.8
S_{sp}, m^2/g	9	33	28	67	75	72	100	100
d_{pore}, nm	330	74	–	101	–	–	11	10

The amount of these compounds was much greater in the preparation of the Ni/Al_2O_3 catalyst by homogeneous precipitation (Fig. 3c); this verified the results of chemical analysis.

The amount of nickel supported onto a corundum honeycomb monolith was greater than that supported onto α-Al_2O_3 rings by a factor of 2.5–3 (Table 1). This was likely due to different geometric shapes and, correspondingly, external geometric surface areas (S_{geom}) of the supports. Indeed, the S_{geom} of the honeycomb monolith (32 cm^2) was greater than the external surface area of the α-Al_2O_3 rings (19 cm^2) by a factor of ~2 at equal sample weights. Note that we did not detect microscopic differences between the surface morphologies of the parent supports.

After supporting Ni, S_{sp} increased by ~30%, whereas it increased by 2–3 orders of magnitude after pyrolysis, as compared with that of the parent support (Table 1). Evidently, this effect was due to the formation of a CFC layer, whose average specific surface area was roughly estimated at 500 m^2/g carbon. The carbon yield for macroporous Al_2O_3 was higher than 70 g/g, which is greater than the value of Y for mesoporous alumina by a factor of 5–10 (Table 1).

Upon supporting Ni onto α-Al_2O_3 by homogeneous precipitation, the amount of synthesized carbon and the carbon yield were found to be higher than those upon impregnation by a factor of 2–3 (Table 1). A visual analysis of cleavages showed that carbon was uniformly synthesized across the entire granule without

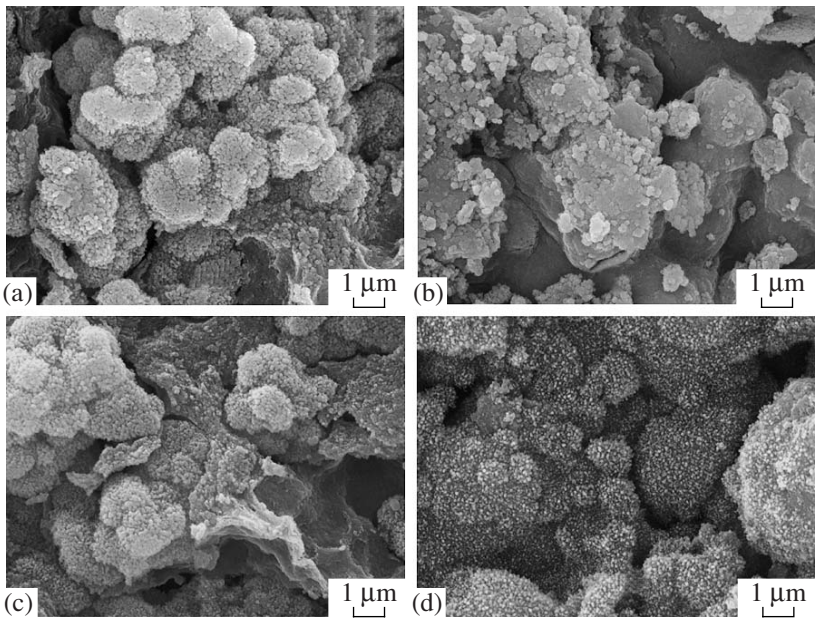

Fig. 2. Electron-microscopic images of the surface of mesoporous θ-Al_2O_3 (rings): (a) the parent support, (b) the support carbonized in the course of pyrolysis without Ni (0.8% carbon), (c) the support carbonized in the course of pyrolysis on a Ni/Al_2O_3 catalyst prepared by impregnation (1.2% carbon), and (d) the support carbonized in the course of pyrolysis on a Ni/Al_2O_3 catalyst prepared by homogeneous precipitation (1.1% carbon).

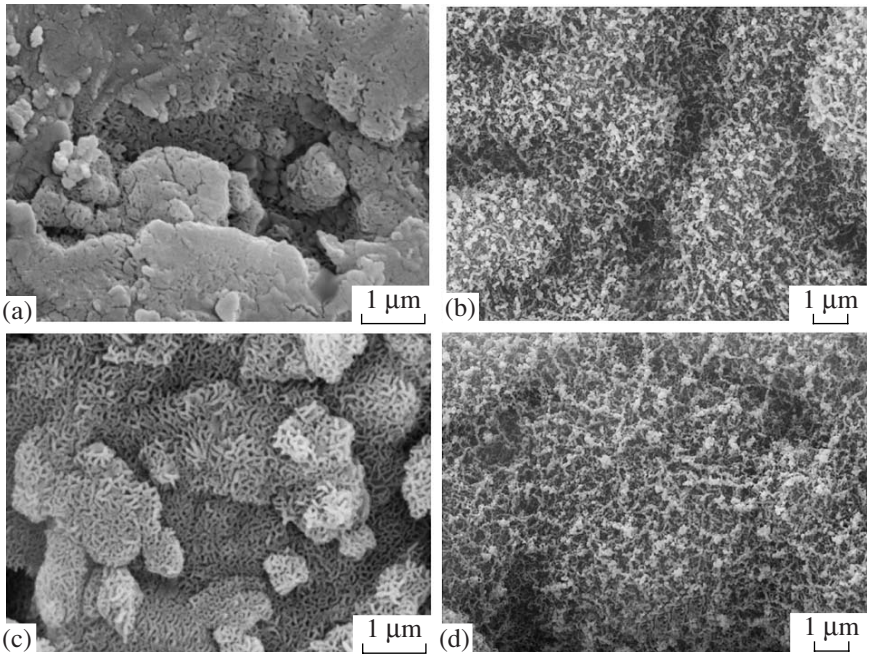

Fig. 3. Electron-microscopic images of the surface of macroporous α-Al_2O_3 (rings): (a) the support with 0.06% Ni supported by impregnation, (b) the support with a CFC layer synthesized on Ni/Al_2O_3 (a), (c) the support with 0.11% Ni supported by homogeneous precipitation, and (d) the support with a CFC layer synthesized on Ni/Al_2O_3 (c).

the formation of a crust region. Note that corundum without supported nickel was inactive under the test conditions of pyrolysis and the surface concentration of pyrolytic carbon was no higher than 0.1%.

As found by the scanning electron microscopic study of the adsorbents, the morphology of a carbon layer synthesized on α-Al_2O_3 did not depend on the procedure used for supporting Ni. The surface layer was formed by the interlacing of relatively long carbon nanofibers (Figs. 3b, 3d). Analogous results were obtained in the study of a CFC layer on the corundum monolith.

Thus, a comparison between the two procedures used for supporting nickel compounds onto the surface of macroporous Al_2O_3 exhibited the following main differences: First, the S_{sp} of the parent support increased most significantly in the synthesis of CFC on Ni supported by homogeneous precipitation. Second, the carbon yield for Ni/Al_2O_3 upon homogeneous precipitation was higher than that for Ni/Al_2O_3 upon impregnation by a factor of ~2 (Table 1).

Based on the experimental data, we can conclude that homogeneous precipitation is preferable for the formation of a Ni/Al_2O_3 catalyst from the standpoint of increasing process productivity of the CFC synthesis.

As mentioned above, a comparative analysis of the texture characteristics of adsorbents with a synthesized carbon layer showed that the macroporous supports were characterized by a considerable (by a few orders of magnitude) increase in the S_{sp} of the supports (from 0.5–6 to 30–80 m^2/g), whereas the specific surface area of mesoporous Al_2O_3 increased only slightly (from 60–80 to 70–100 m^2/g) (Table 1). As will be demonstrated below, the observed differences were due to the texture peculiarities of the CFC layer.

A comparative analysis of pore-size distribution diagrams demonstrated that the pore structures of the parent mesoporous δ-alumina and the adsorbent with a CFC layer were identical (Fig. 4a); d_{pore} = 10–11 nm also remained unchanged (Table 1). In the synthesis of a CFC layer on macroporous α-Al_2O_3, the value of d_{pore} decreased from 330 to 74 nm (Table 1) and mesopores of size 20–50 nm appeared in the pore structure of the adsorbent (Fig. 4b); that is, the macroporous support became an adsorbent with a bidisperse pore structure. An analogous situation was also observed in corundum honeycomb monoliths, in the pore structure of which the diameter of macropores of size ≥200 nm decreased and mesopores of size 40–70 nm appeared (Fig. 4c). The total pore volume supports after the synthesis of CFC insignificantly decreased (by 10–20%). Based on the above results, we can conclude that mesopores 10–50 nm in diameter were predominant in the carbon layer 1 μm or smaller in thickness. As mentioned above, this layer was formed by a chaotic interlacing of thin nanofibers 100–500 nm in length. On the macroporous supports, the CFC layer was synthesized in macro- or supermacropores; as a result, the texture with a bimodal pore-size distribution was formed. In the case of the mesoporous supports, carbon deposits filled the mesopores of Al_2O_3; the pore volume decreased, whereas the pore size remained unchanged.

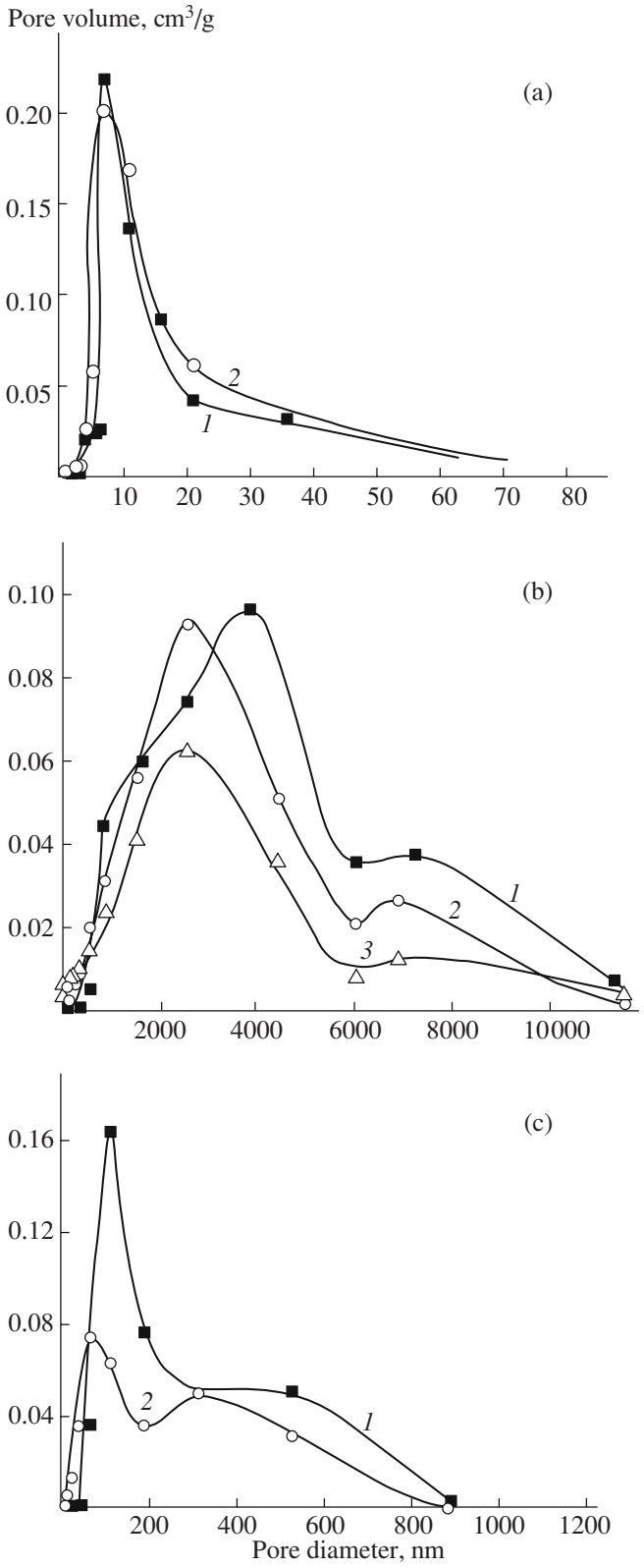

Fig. 4. Pore-size distribution for (a) δ-Al_2O_3, (b) α-Al_2O_3, and (c) a corundum honeycomb monolith: (*1*) parent support; (*2*) adsorbent with a CFC layer of (a) 4.3, (b) 2.95, or (c) 6.4% carbon; and (*3*) adsorbent with a CFC layer of 8.4% carbon (b).

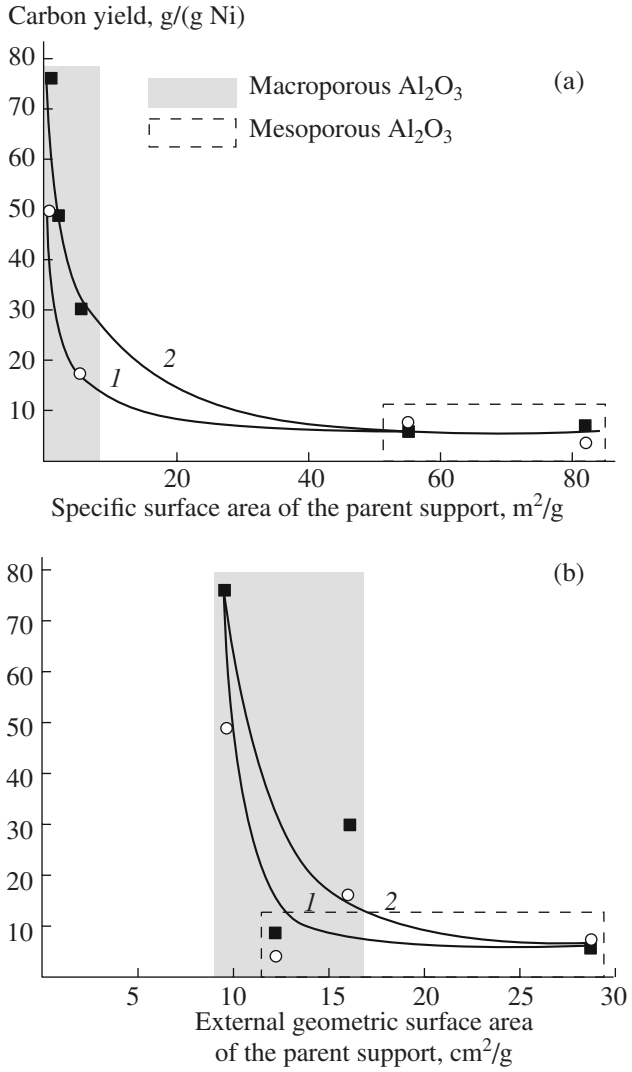

Fig. 5. Dependence of the carbon yield on (a) S_{sp} or (b) S_{geom}. The Ni/Al_2O_3 catalyst was prepared by (*1*) impregnation or (*2*) homogeneous precipitation.

The carbon yield dramatically decreased with the value of S_{sp} of parent supports, which was measured by the BET method (Fig. 5a). An analogous dependence was also observed for the surface concentration of nickel per 1 m^2. However, it is obvious that the surface is not fully accessible to the Ni^{2+} compounds, particularly in the case of mesoporous supports. Assuming that, undoubtedly, the external geometric surface of a support is accessible to large particles of nickel hydroxide formed by homogeneous precipitation, we calculated the surface concentration of nickel per 1 cm^2 of the external geometric surface and the carbon yield (Fig. 5b). The corundum honeycomb monolith was characterized by a maximum concentration of supported nickel (30 μmol/cm^2) and almost complete recovery (~90%) of nickel from solutions in the course of supporting (Table 2). A comparatively high concen-

Table 2. Characteristics of Ni catalysts prepared by homogeneous precipitation onto various alumina modifications

Texture parameters of the parent support		Geometric shape of the support	S_{geom}, cm^2/g	Ni, mg/g	Fraction of supported Ni, %*	Ni, mg/cm^2 (calculated)
S_{sp}, m^2/g	d_{pore}, nm					
0.5	2900	Rings	9.5	1.1	37	0.11
5.5	203	Honeycomb monolith	16	2.7	92	0.17
55	25	Rings	29	1.8	61	0.06
82	21	Rings	12	1.6	54	0.13

* Calculated based on the total amount of Ni^{2+} taken for supporting.

tration of Ni on the rods of mesoporous alumina (Table 2) suggests that the deposition of nickel compounds on the given support occurred not only on the external geometric surface of the granules. Indeed, as noted above, the synthesis of CFC was observed at a depth of ~10% of the granule diameter. As can be seen in Fig. 5b, the carbon yield dramatically decreased with the S_{geom} of parent supports, analogously to the curve in Fig. 5a. To explain the resulting behaviors, the following assumptions can be made: First, the particles of nickel compounds formed on the surface of macroporous supports exhibit a higher specific catalytic activity, which can be explained by both the morphology of the particle and the absence of diffusion limitations on the mass transfer of propane and butane molecules to supported nickel. Consequently, relatively long carbon nanofibers are synthesized on these supports (Figs. 3b, 3d). At the same time, both the diffusion limitations in a pyrolysis reaction and the deactivation of a nickel catalyst because of encapsulation in graphene layers due to the carbonization of the support can occur on mesoporous supports. In this case, the synthesis of CFC terminates at early stages and the carbon deposits on these supports do not exhibit a pronounced fibrous structure (Figs. 2c, 2d). Second, in the granules of macroporous α-Al_2O_3 and in the monolith, carbon is formed uniformly over the entire volume because of the greater accessibility of the surface to Ni, whereas the major portion of the granule surface is out of operation in mesoporous Al_2O_3 and adsorbents with a crust structure are formed.

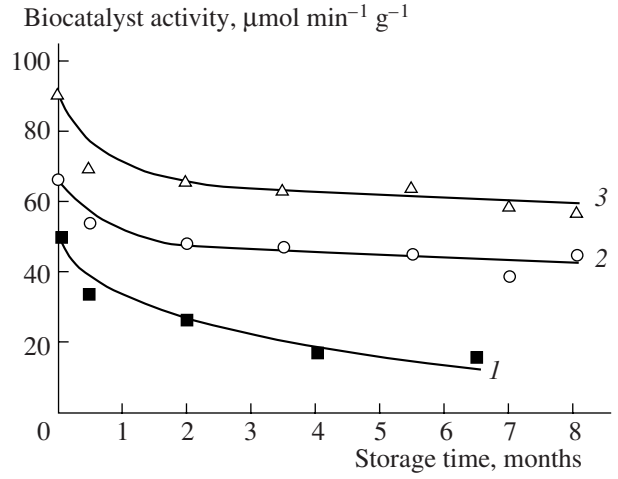

Fig. 6. Activity changes in the long-term storage of heterogeneous biocatalysts prepared by the adsorption of glucoamylase on mesoporous δ-Al_2O_3: (*1*) with no carbon layer, (*2*) with a CFC layer (2.3% carbon), (*3*) with a carbon layer additionally treated with hydrogen (4.3% carbon). Conditions for the determination of activity: 50°C; 0.05 M acetate buffer solution, pH 4.6; 3% dextrin solution; flow rate through a biocatalyst bed, 30 ml/min. Storage conditions: 18–20°C; 0.05 M acetate buffer solution, pH 4.6.

PRACTICAL APPLICATIONS

Adsorptive Immobilization of the Enzyme Glucoamylase

We studied the effect of the physicochemical characteristics of the carbon layer synthesized on alumina on the properties of heterogeneous biocatalysts for the hydrolysis of dextrin. We found that glucoamylase adsorbed on carbon-containing mesoporous δ-Al_2O_3 exhibited an enzymatic activity that was higher than that of glucoamylase adsorbed on macroporous α-Al_2O_3 by a factor of 3; in this case, the given supports were almost identical to each other in terms of adsorption properties. We also found that glucoamylase adsorbed on noncarbonized δ-Al_2O_3 in insignificant amounts, although the biocatalyst exhibited a comparatively high enzymatic activity (Fig. 6, curve *1*). Thus, the activity of glucoamylase adsorbed on a white (noncarbonized) parent support was higher than the activity of this enzyme on a black (carbonized) adsorbent by one order of magnitude. The higher activity of the biocatalyst prepared by the adsorption of glucoamylase on the rods of mesoporous δ-Al_2O_3 with a crust structure nonuniformly coated with CFC can be explained based on the following reasons: First, glucoamylase adsorbed within the inner light region of granules, where, as noted above, the enzyme exhibits a higher specific enzymatic activity, made a considerable contribution to the activity of the biocatalyst. Second, the occurrence of long chaotically interlaced carbon nanofibers synthesized on macroporous α-alumina (Figs. 3b, 3d) created diffusion hindrances for the mass transfer of

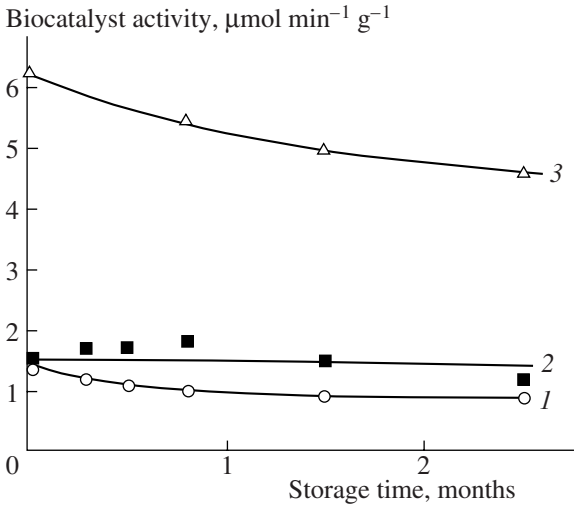

Fig. 7. Activity changes in the long-term storage of heterogeneous biocatalysts prepared by the adsorption of yeast cells with invertase activity on CFC-containing (*1*) aluminosilicate, (*2*) cordierite, and (*3*) corundum honeycomb monoliths. Conditions for the determination of activity: 50°C; 0.05 M acetate buffer solution, pH 4.6; 20% white sugar solution; flow rate through a biocatalyst bed, 30 ml/min. Storage conditions: 18–20°C; 0.05 M acetate buffer solution, pH 4.6.

a high-molecular-weight substrate—dextrin (MW 3000–5000 Da)—to the immobilized enzyme.

After additional treatment of the CFC layer with hydrogen, surface hydroxy groups were reduced and the hydrophobicity of the support increased. In this case, the adsorption and activity of the biocatalyst increased only slightly (by 10–20%) (Fig. 6, curve *3*). Consequently, taken alone, the CFC layer exhibits optimum hydrophilic–hydrophobic properties and its additional treatment (reduction with hydrogen or oxidation in boiling nitric acid) does not affect significantly the properties of the resulting biocatalysts, as supported by the results obtained previously [12].

The stability of heterogeneous biocatalysts was enhanced upon the immobilization of glucoamylase on the surface of CFC-containing adsorbents, as compared with that of the parent supports. Thus, the glucoamylase on CFC/Ni/δ-Al_2O_3 biocatalysts retained up to 80% of their initial activity after storage for 8–12 months at 20–22°C (Fig. 6, curves *2* and *3*), whereas the glucoamylase on δ-Al_2O_3 biocatalysts lost 50% activity within 2–3 months (Fig. 6, curve *1*). It is likely that the enzyme was immobilized more strongly in the CFC layer because of multipoint interaction in mesopores with the appropriate size.

Adsorptive Immobilization of Nongrowing Baker's Yeast Cells

For the adsorption of bulky biological objects such as yeast cells (to 6 μm), we used supports as honeycomb monoliths with transport channels of ~0.5–1 mm, which were prepared based on aluminosilicates and Al_2O_3. On the surface of these supports, CFC layers were synthesized under the conditions described above. The tested supports did not differ in terms of the amount and tightness of adsorption of baker's yeast cells. The biocatalysts prepared by the adsorption of microorganisms on these monoliths were also equally

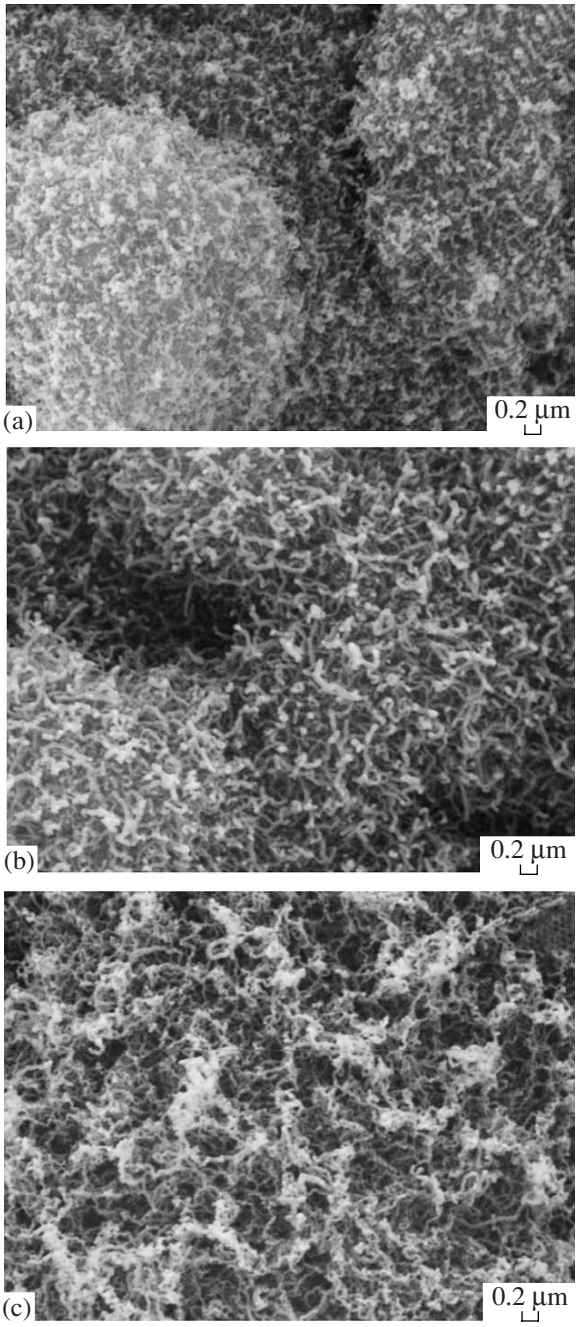

Fig. 8. Electron-microscopic images of a CFC layer synthesized on (a) corundum (9.5% carbon), (b) aluminosilicate (4.4% carbon), and (c) cordierite (1.3% carbon) honeycomb monoliths.

stable (Fig. 7): 80–90% of the initial activity was retained after storage for 2–3 months at 20–22°C. The prepared biocatalysts differed most significantly in enzymatic activity. As can be seen in Fig. 7, yeast cells immobilized on a CFC-containing corundum monolith were more active than the cells on aluminosilicate monoliths with a CFC layer by a factor of 5–6. The found differences in the activity of biocatalysts can be explained by the presence or absence of diffusion limitations in the reaction of sucrose inversion. Indeed, an analysis of pore-size distribution diagrams demonstrated that d_{pore} = 100 nm in the pore structure of CFC-containing corundum monoliths, whereas d_{pore} is ~40–50 nm in aluminosilicate monoliths with a CFC layer. Using scanning electron microscopy, we found that the CFC layer on corundum supports was formed by the interlacing of shorter nanofibers (Fig. 8a) than those in the aluminosilicate monoliths (Figs. 8b, 8c). Consequently, the diffusion of a substrate (sucrose) to yeast cells immobilized on CFC-containing aluminosilicate monoliths limited the heterogeneous process of sucrose inversion.

CONCLUSIONS

We found that the use of homogeneous precipitation for the preparation of Ni/Al_2O_3 catalysts for the pyrolysis of hydrocarbons, which results in the synthesis of carbon nanofibers on the support surface, is more effective than impregnation from the standpoint of increasing the process productivity of CFC synthesis. Thus, the carbon yield in the homogeneous precipitation of Ni^{2+} compounds is higher than that in impregnation, on average, by a factor of ~2; consequently, the amount of synthesized carbon is greater. We found that the morphology of a synthesized carbon layer depends on the texture characteristics of the parent alumina, and it is independent of the procedure used for supporting nickel compounds. On mesoporous Al_2O_3, carbon deposits are synthesized without a well-defined fibrous structure, whereas carbon nanofibers ~500 nm in length are synthesized on macroporous alumina. In this case, the CFC is synthesized on macroporous supports uniformly across a support granule or a honeycomb monolith wall, whereas adsorbents with a crust structure can be prepared based on mesoporous supports.

We found that, regardless of the procedure of supporting Ni, the carbon yield dramatically decreased (by an order of magnitude) as the texture of parent supports changed from macroporous to mesoporous. This was likely due to differences in the catalytic activity and possible deactivation (coking) of the Ni/Al_2O_3 catalyst.

We found that, in the synthesis of a carbon layer, the texture characteristics of mesoporous alumina changed only slightly, whereas a considerable change in the texture of adsorbents was characteristic of macroporous supports. Thus, in the synthesis of CFC, the specific surface area of macroporous supports increased by more than one order of magnitude; mesopores appeared in the pore structure along with macropores (because of the interlacing of carbon nanofibers), and the pore structure of the adsorbents became bidisperse.

We demonstrated that adsorbents with a CFC layer are promising supports for the adsorptive immobilization of enzymatically active substances—enzymes and microorganisms. Thus, heterogeneous biocatalysts prepared by the adsorption of glucoamylase on carbon-containing aluminum oxides and by the adsorption of nongrowing baker's yeast cells on a CFC-containing corundum honeycomb monolith exhibited high enzymatic activity and stability in the biocatalytic processes of dextrin hydrolysis and sucrose inversion, respectively.

ACKNOWLEDGMENTS

This work was supported by the Presidium of the Siberian Branch of the Russian Academy of Sciences (integration project no. 4.4).

REFERENCES

1. Chesnokov, V.V., Zaikovskii, V.I., Buyanov, R.A., et al., *Kinet. Katal.*, 1994, vol. 35, no. 1, p. 145.
2. Buyanov, R.A. and Chesnokov, V.V., *Khim. Interes. Ust. Razv.*, 1995, vol. 3, no. 3, p. 177.
3. Buyanov, R.A. and Chesnokov, V.V., *Zh. Prikl. Khim.*, 1997, vol. 70, no. 6, p. 978 [*Russ J. Appl. Chem.* (Engl. Transl), vol. 70, no. 6, p. 935].
4. Fenelonov, V.B., Derevyankin, A.Yu., Okkel, L.D., et al., *Carbon*, 1997, vol. 35, no. 8, p. 1129.
5. Kuvshinov, G.G., Mogilnykh, Yu.I., Kuvshinov, D.G., et al., *Carbon*, 1998, vol. 36, nos. 1–2, p. 87.
6. Vieira, R., Ledoux, M.-J., and Pham-Huu, C., *Appl. Catal., A*, 2004, vol. 274, nos. 1–2, p. 1.
7. Reshetenko, T.V., Avdeeva, L.B., Ismagilov, Z.R., et al., *Carbon*, 2003, vol. 41, no. 8, p. 1605.
8. Avdeeva, L.B., Reshetenko, T.V., Ismagilov, Z.R., et al., *Appl. Catal., A*, 2002, vol. 247, no. 1, p. 53.
9. de Lathouder, K.M., Bakker, J., Kreutzer, H.T., et al., *Chem. Eng. Sci.*, 2004, vol. 59, nos. 22–23, p. 5027.
10. De Lathouder, K.M., Flo, T.M., Kapteijn, F., and Moulijn, J.A., *Catal. Today*, 2005, vol. 105, nos. 3–4, p. 443.
11. Kovalenko, G.A., Perminova, L.V., Plaksin, G.V., et al., *Prikl. Biokhim. Mikrobiol.*, 2006, vol. 42, no. 2, p. 163 [*Appl. Biochem. Microbiol.* (Engl. Transl), vol. 42, no. 2, p. 145].
12. Kovalenko, G.A., Perminova, L.V., Khomov, V.V., et al., *Biotekhnologiya*, 2004, no. 6, p. 34.